

# Theoretical and Experimental Investigations of a Passively Mode-Locked Nd: Glass Laser

C. Kolmeder and W. Zinth

Physik Department der Technischen Universität München, D-8000 München,  
Fed. Rep. Germany

Received 5 December 1980/Accepted 15 December 1980

**Abstract.** The presented theoretical model for a mode-locked Nd-glass laser simultaneously takes into account dynamics of the mode-locking dye, amplification saturation and radiation background. A systematic variation of laser parameters gives insight into the pulse formation process and allows to improve the laser design. The calculations show that it should be possible to decrease considerably the duration of light pulses of a mode-locked Nd-glass laser. Using a new mode-locking dye with a switching time of  $\tau = 2.7 \times 10^{-12}$  s we obtained stable laser operation and a pulse duration of  $1.7 \times 10^{-12}$  s.

**PACS:** 42.55

High peak intensities and pulse durations of picoseconds combined with remarkable spectral properties make mode-locked neodymium-glass lasers well suited for the study of ultrashort processes. Numerous experimental and theoretical investigations of the pulse formation process in mode-locked Nd-glass lasers have been published [1–13]. It has been recognized quite early that the important pulse properties may fluctuate and critically depend on the specific resonator configuration. The theoretical models have introduced step by step the different mechanisms determining the pulse formation. In general, the existing theoretical literature on mode-locked solid-state lasers treats idealized laser systems. Until now the dynamics of the mode-locking dye and the radiation background were not considered at the same time. These parameters are important to the experimentalist intending to design a reliable mode-locking Nd-glass laser.

In this paper we study a mode-locked Nd-glass laser theoretically as well as experimentally. In a first part we develop a realistic mode-locking model. It takes into account the starting radiation pattern, the dynamics of the mode-locking dye, and the saturation of the amplification. A numerical calculation is performed for a variety of laser parameters. In the experimental part we study the influence of various switching

dyes on mode-locking and compare experimental and calculated values of the pulse duration.

## 1. Theory

We briefly review the formation of ultrashort light pulses in a mode-locked solid-state laser [5, 9, 12]. At the beginning of laser action spontaneous fluorescence is amplified by the optically pumped laser rod and reduced by the resonator losses. Since light intensity and light energy are small only the linear optical parameters are important. This early period of pulse development is called the linear stage of amplification. The following nonlinear stage starts when the light intensity becomes strong enough for saturation effects to occur. Bleaching of the absorbing dye and amplification saturation favor the most intense pulse, reduce the background and shorten the final pulse. The growth of light intensity ends when the amplification decreases. Finally, the resonator losses prevail and the pulse energy decreases.

### 1.1. The Linear Amplification Stage

The linear stage is well described by a simplified model considering only linear loss and linear amplification. The loss is produced by the output mirror and the

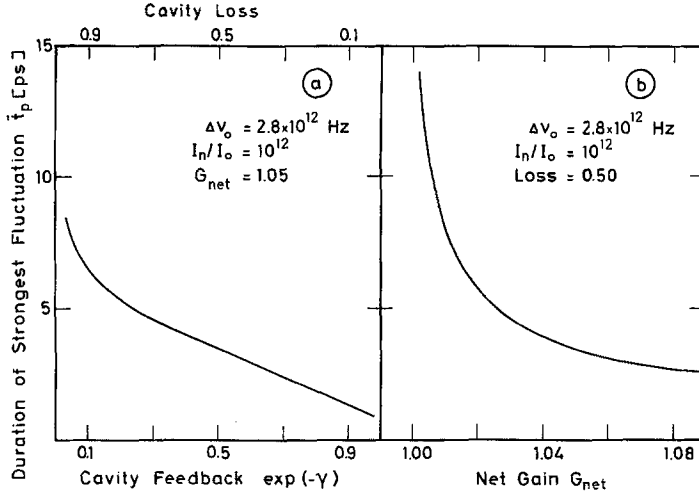


Fig. 1. Duration of the strongest fluctuation ( $\bar{N}=1$ ) in the linear stage after amplification by  $10^{12}$ . A width of the inhomogeneously broadened laser transition  $\Delta\nu_0 = 2.8 \times 10^{12}$  Hz ( $\Delta\tilde{\nu}_0 = 93 \text{ cm}^{-1}$ ) is assumed. (a) The pulse duration plotted as a function of the cavity loss for a net gain at the end of the linear stage  $G_{\text{net}} = 1.05$ . (b) The pulse duration as a function of the net gain for a constant cavity loss of 50 %

mode-locking dye. It is constant within the bandwidth of laser emission. The amplification in the laser rod is frequency dependent. Due to the optical pumping the amplification increases slowly up to the end of the linear stage. The important parameters in the linear stage are the spectral shape of the fluorescence emission, the growth of the amplification and the amount of linear losses per round trip.

The starting condition of the laser process is spontaneous fluorescence from the inhomogeneously broadened laser transition. Interference of resonator modes at different spectral positions leads to a fluctuating light intensity within the resonator. The mean duration  $t_p$  of the light bursts is determined by the width  $\Delta\nu_0$  of the fluorescence curve [14, 15]. For Nd:phosphate glass  $t_p$  is approximately  $10^{-13}$  s. When the pumping process continues the gain near the peak of the fluorescence curve will overcome the losses and light along the resonator axis is amplified (first threshold). The light intensity at frequency  $\nu$  after the  $n^{\text{th}}$  transition  $I_n(\nu)$  is calculated from the starting intensity  $I_0(\nu)$  and the normalized line shape  $F(\nu)$  of the fluorescence curve

$$I_n(\nu) = I_0(\nu) \exp \left[ F(\nu) \sum_{m=0}^n g(m) - \gamma n \right], \quad (1)$$

where  $g(m)$  is the total gain coefficient at the  $m^{\text{th}}$  transition through the resonator and  $\gamma$  is the gain at lasing threshold,  $\gamma = -\ln(1 - \text{linear loss})$ . In our model the gain coefficient  $g(m)$  is held constant during one round trip through the resonator and afterwards it is increased by a constant amount. This linear growth of the gain is justified when the duration of the flash lamp pulse is much longer than the linear state. In general, the net amplification  $I_{m+1}/I_m$  in the linear stage is small and restricted to a narrow frequency band around the peak of the fluorescence, (1). Assuming a

Gaussian shape of the fluorescence curve we calculate the narrowed bandwidth  $\Delta\nu_n$  of the light pulse after the  $n^{\text{th}}$  transition:

$$\Delta\nu_n = \Delta\nu_0 [1 + n\gamma + \ln(I_n/I_0)]^{-1/2}, \quad (2)$$

$$n = \frac{2 \ln(I_n/I_0)}{\ln(G_{\text{net}})}. \quad (3)$$

As starting bandwidth  $\Delta\nu_0$  we use the halfwidth (FWHM) of the fluorescence curve. The number of round trips  $n$  in (3) is a function of the total intensity increase  $I_n/I_0$  and the net gain after the  $n^{\text{th}}$  transition  $G_{\text{net}} = \exp[g(n) - \gamma]$ . The bandwidth  $\Delta\nu_n$  decreases when the total amplification  $I_n/I_0$ , the number of round trips  $n$  or the linear losses  $\gamma$  will grow. For  $I_n/I_0$  held constant the number of round trips becomes larger when a smaller end amplification  $G_{\text{net}}$  is used.

In the linear stage we treat the radiation within the resonator as a Gaussian noise from a narrow band source with halfwidth  $\Delta\nu_n$ . From statistical considerations one deduces the mean duration  $\bar{t}_p$  (FWHM) and the mean frequency  $\bar{N}$  of fluctuations exceeding the average intensity  $\bar{I}$  by a factor  $\beta$  [5], i.e.

$$\bar{t}_p = 1/(\Delta\nu_n \sqrt{\beta}), \quad (4)$$

$$\bar{N} = \Delta\nu_n \sqrt{2\beta} \exp(-\beta). \quad (5)$$

Figure 1 shows the mean duration of the most intense pulse.  $\bar{t}_p$  is calculated from (1) to (5) using an intensity increase  $I_n/I_0 = 10^{12}$ , a frequency width of the fluorescence curve  $\Delta\nu_0 = 2.8 \times 10^{12}$  Hz ( $93 \text{ cm}^{-1}$ ), and a cavity round-trip time of  $1 \times 10^{-8}$  s. In Fig. 1a, a constant net gain at the end of the linear stage,  $G_{\text{net}} = 1.05$ , is assumed and the linear loss is varied. During the linear stage the pulses always become longer, e.g. for a loss of 50 % the pulse duration is increased from 0.16 ps to 3.4 ps. Figure 1b shows the pulse duration for a constant loss of 50 % when the net gain  $G_{\text{net}}$  is varied. For a

small net gain of 1.005 the linear stage persists for many round trips,  $n \approx 10^4$ , and the pulses become longer than  $10^{-11}$  s. The shortest pulse durations are found for a high net gain and a high cavity feed-back (low loss).

### 1.2. The Nonlinear Stage of Amplification

In the nonlinear stage the coupling of the resonator modes changes the radiation pattern. The noisy radiation inside the cavity, with many fluctuations and small peak-to-background ratio, is drastically changed. A single short light pulse on a small background is generated. In a passively mode-locked Nd-glass laser the mode-locking is caused by saturation of absorption and amplification [9, 10, 12].

We treat the propagation of light through the switching dye with the equation of two-level systems and the wave equation. We do not consider coherent propagation of light as well as contributions from orientational motion of dye molecules:

$$\frac{\partial N}{\partial t} = \frac{-2I\sigma_a N}{h\nu} + \frac{M-N}{\tau}, \quad (6)$$

$$\frac{\partial I}{\partial t} + \frac{c}{\eta} \frac{\partial I}{\partial x} = -\frac{c}{\eta} I\sigma_a N. \quad (7)$$

$M$  denotes the density of dye molecules with absorption cross section  $\sigma_a$ , with ground state recovery time  $\tau$ , and with transition energy  $h\nu$ .  $N$  is the difference of population density between the lower and the upper level.  $\eta$  is the refractive index and  $c$  the velocity of light. Equation (6) describes the population changes of the dye according to absorption, to stimulated emission, and to spontaneous decay. On the other hand, (7) shows the transmission of the light pulse with an intensity distribution  $I(x, t)$ . Pulses with small intensities,  $I \ll I_S = h\nu/2\sigma_a\tau$ , experience linear absorption, whereas pulses with high intensities,  $I \gg I_S$ , are transmitted with almost no change in amplitude or shape. Only for pulse intensities close to the saturation intensity ( $0.1 I_S < I < 10 I_S$ ) the peak is transmitted with smaller loss than the wings and a pulse shortening results. In the literature most model calculations of mode-locked solid-state lasers used the approximation of long pulses,  $t_p \gg \tau$ , or short pulses,  $t_p \ll \tau$ , where the transmission through the dye depends only on intensity or energy, respectively, and may be described analytically. Both conditions  $t_p \gg \tau$  and  $t_p \ll \tau$ , are not fulfilled for mode-locked Nd-glass lasers where one can obtain  $t_p \approx 5$  ps for dyes with  $\tau \approx 7$  ps.

The calculations of the frequency dependent amplification are performed in the frequency domain. The peak amplification  $\exp[g(n)]$  during the  $n^{\text{th}}$  transition can be calculated from the previous gain  $g(n-1)$  and

the depletion due to the density of photons  $P(n-1)$  produced in the previous transition.

$$g(n) = \sigma_e l N(n) = g(n-1) - \sigma_e l P(n-1), \quad (8)$$

where  $\sigma_e$  is the cross section of stimulated emission,  $l$  is the length of the amplifying medium and  $N(n)$  represents the density of population inversion of the laser transition.

According to (8) the decrease of amplification (saturation) depends on the energy of the produced light. At the beginning of the nonlinear stage most saturation is induced by the many fluctuations with small intensities, see (4) and (5) with  $\beta \approx 1$ . When the background is suppressed the remaining pulse produces negligible saturation. Finally, at a high intensity, it experiences self-phase modulation by the nonlinear refractive index  $n_2$  of the laser glass. When the nonlinear path  $\Delta x_{NL} = \int I(x)n_2(x)dx$  exceeds  $\Delta x_{NL} > 0.3 \mu\text{m}$ , the broadening of the pulse spectrum is strong enough to reduce further amplification [16–18].

## 2. Model Calculations of Mode-Locking

Our computations are made as follows: The starting conditions supplied by the linear stage of amplification are Gaussian shaped pulses with mean peak intensities and mean pulse durations according to (2) to (5). In order to study single pulse formation and background suppression we chose six groups representing light pulses of different peak intensities. The number of pulses in every group is calculated to give the true total light energy. The pulses are Fourier transformed into the frequency domain; they are amplified according to (8) and Fourier synthesized. Between the amplifying medium and the mode-locking dye the light intensity is changed by a factor  $F$  resulting from a focussing or defocussing telescope. We introduce the intensity ratio  $F = I_{\text{abs}}/I_{\text{amp}}$ , where  $I_{\text{abs}}$  and  $I_{\text{amp}}$  are the intensities in the switching dye and in the amplifier, respectively. The subsequent propagation through the absorber is computed with (6) and (7). After each round trip the density of photons produced is calculated and the parameters of amplification are readjusted. In Tables 1a and b we compiled the parameters of laser glass and mode-locking dyes, respectively.

The following points should be noted: (i) The influence of the background and the limited switching speed of the dye require a numerical computation of pulse propagation. (ii) Our model concentrates on single-pulse operation, background suppression, and pulse duration at a certain intensity level. The nonlinear processes at the very end of the pulse formation stage are not considered in detail. In the experiment we select one pulse from the leading part of the pulse train

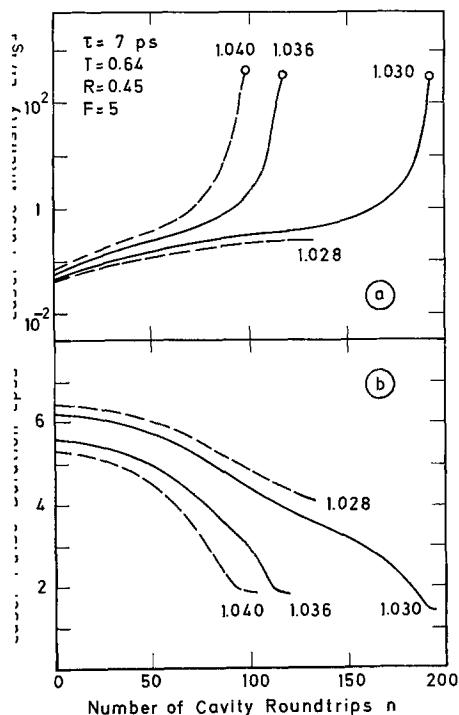


Fig. 2. Development of the strongest fluctuation in the nonlinear stage for dye I,  $T=64\%$ ,  $\tau=7$  ps, mirror reflectivity  $R=45\%$ , and focussing  $F=I_{\text{abs}}/I_{\text{amp}}=5$ . The solid curves indicate single pulse operation at the end of the pulse formation stage. The circles show the intensity level where self-phase modulation in the glassrod becomes important. (a) Peak intensity in the absorbing dye versus number of round trips for different starting net gains. (b) Pulse duration versus number of round trips. The most effective pulse shortening is found at the second threshold,  $G_{\text{net}}=1.030$ .

and the exact reproducibility of the shape of the pulse train is of little importance. (iii) Our model does not respect shot-to-shot variations of the starting radiation pattern. The fluctuations of the starting conditions have been studied in detail in the literature [9–12].

### 2.1 Variation of the Net Amplification $G_{\text{net}}$

The main characteristics of pulse formation can be seen when we vary the net gain at the end of the linear stage. In a real experiment this can be done by adjusting the energy supplied to the flash-lamp circuit.

Figure 2 shows the results for the absorbing dye I ( $\tau=7$  ps) with transmission  $T=64\%$  and mirror reflectivity  $R=45\%$ . The light intensity in the laser rod is smaller than the intensity in the dye by a factor of five,  $F=I_{\text{abs}}/I_{\text{amp}}=5$ . In Fig. 2a the intensity of the strongest fluctuation within the absorbing dye is plotted as a function of the number of round trips  $n$ . The initial conditions are calculated according to (1) to (5). For small values of the net gain, e.g.  $G_{\text{net}}=1.028$ , the peak

intensity first grows slowly and reaches a broad maximum near  $I_M \approx 0.1 \times I_S$ . During the nonlinear stage the background consumes the energy stored in the laser rod. Even the most intense pulse does not reach an intensity level to bleach sufficiently the absorbing dye. No mode-locking takes place. When the net gain is increased slightly, e.g. up to 1.030, the pulse development at the beginning of the nonlinear stage is very similar. The most intense fluctuation reaches a slightly higher intensity level before saturation of the amplification takes place. A long competition between bleaching the dye and saturation of the amplification takes place. Only one, the most intense fluctuation experiences a net amplification whereas the background, initially containing most of the light energy, is reduced. During this long period the pulse passes many times through the saturable absorber and a very effective shortening of the pulse results (Fig. 2b). Further amplification stops when the nonlinear properties of the laser components become important (circle on the calculated curves). The lowest value of amplification, where mode-locking is realized, is called the “second threshold” [9, 12]. A further increase of the net gain, e.g. up to 1.036, shows two different results: the higher net gain shortens the linear and nonlinear amplification stage. Our calculation starts with shorter pulse durations but pulse shortening is less efficient in the nonlinear stage. Combining these two effects we get a small increase of the pulse duration. When  $G_{\text{net}}$  exceeds 1.036 the saturation of amplification is not so effective to discriminate all the smaller pulses. A second pulse may bleach the dye (broken line in Fig. 2 with  $G_{\text{net}}=1.040$ ). Selecting pulses just above the second threshold we find single pulse operation. The pulse duration varies between 1.5 ps and 1.8 ps. It should be mentioned once more that our treatment uses the mean statistical distributions. In real lasers stronger variations of pulse durations may occur.

### 2.2 Variation of Linear Resonator Losses

Using higher resonator losses while keeping the net gain constant we have to increase the amplification with consequences on the linear and nonlinear stage. The exact reaction of the system has to be calculated. For our example we have in mind a Nd-glass laser with the following parameters: Low intensity transmission of the dye I,  $T=64\%$ , and focussing  $F=I_{\text{abs}}/I_{\text{amp}}=5$ . The results of our calculations are shown in Fig. 3a. The vertical solid lines indicate the range of pulse durations for the specific output mirrors, when single pulse operation occurs. The dash-dotted line limits this region at the second threshold, whereas at the broken

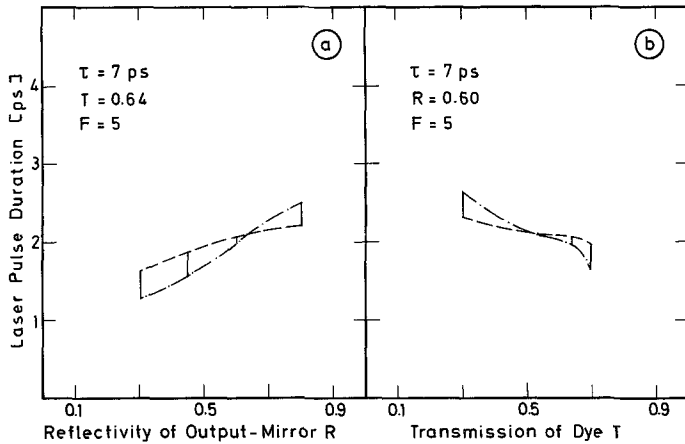


Fig. 3. Pulse duration at the end of the nonlinear stage as a function of (a) the output mirror reflectivity  $R$  and (b) the dye transmission  $T$ . The dash-dotted curve determines the second threshold and the broken curve the boundary between single and double pulse operation

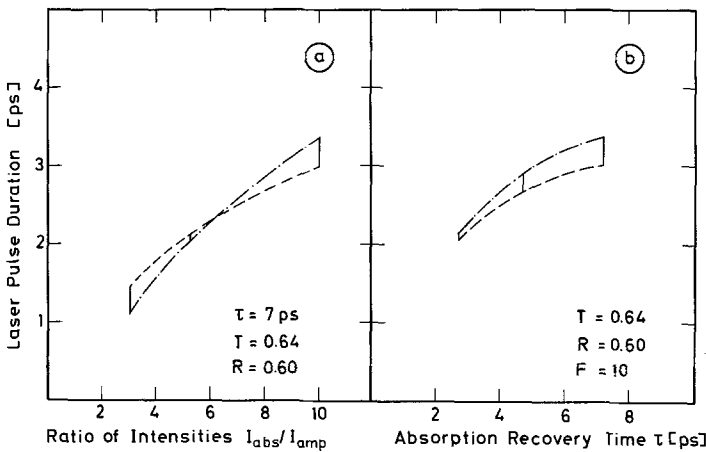


Fig. 4. Pulse duration at the end of the nonlinear stage as a function of (a) the focussing ratio  $F = I_{\text{abs}}/I_{\text{amp}}$  and (b) the absorption recovery time  $\tau$ . Focussing ratio and recovery time are of major importance for laser pulse durations. Small focussing and/or fast absorption recovery times of the mode-locking dye will favor short pulse durations

line double-pulse operation sets in. The pulse durations become shorter when the linear loss is increased. Simultaneously, a wider spread of the pulse durations results. When the reflectivity  $R$  is decreased the net gain at the second threshold increases drastically limiting the useful range of reflectivities. Very interesting is the region near  $R = 70\%$  where the two boundaries of single-pulse operation cross. Under these conditions one expects small fluctuations of the pulse durations.

### 2.3 Variation of the Dye Transmission

Another important parameter for mode-locked lasers is the (low intensity) transmission  $T$  of the nonlinear absorber. The calculations are performed for a reflectivity of the output mirror  $R = 60\%$ , dye I with  $\tau = 7 \text{ ps}$  and  $F = I_{\text{abs}}/I_{\text{amp}} = 5$  (Fig. 3b). The pulse becomes shorter, when the transmission is increased. It should be mentioned that the dye transmission cannot be increased arbitrarily as it leads to poorer mode-locking; e.g., when a low intensity transmission  $T = 80\%$  is used, multiple pulse operation is found.

### 2.4 Intensity Variation in the Mode-Locking Dye

The previous discussion has shown that best mode-locking occurs when the amplification and absorption saturate simultaneously. Within the laser, the range of saturation depends on the cross sections and time constants of amplification and absorption, i.e. it depends on the type of laser glass and mode-locking dye. Specific properties of the resonator such as focussing between amplifier and absorber may be used to adjust the intensity levels.

Figure 4a shows that the shortest pulse durations ( $t_p \approx 1.2 \text{ ps}$ ) are found when the intensity in the dye is small, i.e. when the saturation process in the amplifying glass rod starts early. It should be mentioned that a higher level of amplification is required for the small values  $F = I_{\text{abs}}/I_{\text{amp}}$  e.g. at the second threshold  $G_{\text{net}} = 1.05$  is found for  $F = 3$ , whereas  $G_{\text{net}} = 1.02$  is suitable for  $F = 5$ .

### 2.5 Variation of the Switching Time of the Mode-Locking Dye

The absorption recovery time  $\tau$  of the mode-locking dye is crucial for pulse-shortening. When the switching

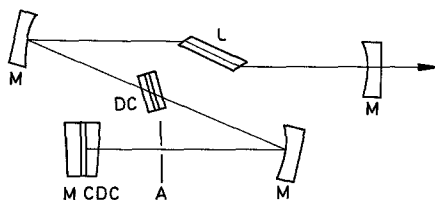


Fig. 5. Schematic of the experimental set-up of the mode-locked Nd-glass laser with mirrors M, laser glass L, contacted dye cell CDC, dye cell DC, and aperture A

time of the absorber in a mode-locked laser is reduced one would expect qualitatively that the pulses are shortened more effectively. The shorter switching time and the higher saturation intensity  $I_s = hv/2\sigma_a\tau$  contribute to pulse shortening. The influence of the different switching times is shown in Fig. 4b, where we calculate the pulse duration as a function of the absorption recovery time  $\tau$  for constant absorption cross section  $\sigma_a$ . It is evident that the shortest pulses occur when the dye with the fastest time constant is used. The parameters in the calculations are  $T=0.64$ ,  $R=0.60$ , and  $F=10$ .

### 3. Experimental

A systematic experimental test of a theoretical model of mode-locking imposes a number of difficulties. In general, the variation of one experimental parameter requires a new alignment of the laser, and changes of pulse properties may sometimes be caused by the alignment procedure. To overcome these difficulties we study in the following the influence of different mode-locking dyes where we have to readjust only the power supplied by the flashlamps.

The set-up of the laser is shown schematically in Fig. 5. We used a curved output mirror with reflectivity  $R=60\%$  and curvature of  $r=3\text{m}$ . The amplifying medium was a 130 mm long Nd-doped glass-rod LG 703, cut under the Brewster angle. Two curved mirrors ( $r=0.5\text{m}$ ) are used to form a region of high light intensity within the resonator. Here, the cell with the switching dye was inserted at Brewster angle. Adjusting the dye cell between the mirrors allowed to increase the light intensity in the mode-locking dye. In our experiment the increase of intensity was chosen to be ten. A flat mirror,  $R=100\%$ , with a contacted dye cell (thickness  $20\ \mu\text{m}$ ) formed the cavity. In most of the experiments described here this cell was only filled with the pure solvent 1,2-dichloroethane. Transverse mode-selection to TEM<sub>00</sub> operation was achieved by the aperture A. An electro-optical shutter (Kerr cell with laser triggered spark gap) was used to select one pulse from the pulse train. The energy of the selected pulse was set to be a factor of four below the pulse energy at the peak of the pulse train. We measured the duration of a single pulse with the second harmonic beam technique [21]. The spatial distribution of the second harmonic light produced in a non-collinear geometry gives the autocorrelation function. The autocorrelation track is detected for each single pulse with an optical multichannel analyser. The duration of the pulse was determined from the width of the autocorrelation track assuming a Gaussian shape of the pulse.

In the experiment we studied three mode-locking dyes (Table 1b). With dye I ( $\tau=7\text{ps}$ ) used in the contacted dye cell (single-pass transmission  $T_0=80\%$ , the cell between the curved mirrors was filled with pure sol-

Table 1a. Properties of the amplifying medium [15]

| Laser glass | Fluorescence lifetime | Fluorescence width (fitted) $\Delta\nu_0/c$ | Cross section of stim. emission $\sigma_a$ | Nonlinear refraction $n_2$       | Length $l$ |
|-------------|-----------------------|---|--|----------------------------------|------------|
| LG 703      | 240 $\mu\text{s}$     | 93 $\text{cm}^{-1}$                         | $4.1 \times 10^{-20} \text{cm}^2$          | $1.1 \times 10^{-13} \text{esu}$ | 20 cm      |

Table 1b. Properties of the mode-locking dyes [19, 20]

| Dye  | Switching time $\tau$ [ps] | Absorption cross section $\sigma_a$ [ $\text{cm}^2$ ] | Saturation intensity $I_s = hv/2\sigma_a\tau$ [MW/ $\text{cm}^2$ ] |
|--|----------------------------|---|--|
| I No. 9860 in 1-2-dichloroethane                                 | $7 \pm 1$                  | $3.7 \times 10^{-16}$                                 | 36   |
| II No. 9860 in 1-2-dichloroethane with Tetrabutyl-ammoniumiodide | $4.7 \pm 1$                | $(3.7 \times 10^{-16})$ assumed                       | (54)   |
| III No. 5 in 1-2-dichloroethane                                  | $2.7 \pm 0.2$              | $(3.7 \times 10^{-16})$ assumed                       | (93)   |

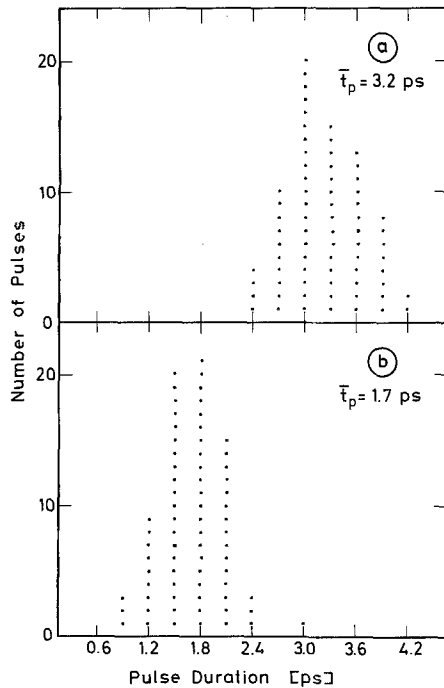


Fig. 6. Histogram of the laser pulse durations for two different mode-locking dyes: (a) Dye Eastman 9860 dissolved in dichloroethane, dye I, ( $\tau = 7$  ps) produces a mean pulse duration of 3.2 ps. (b) Dye No. 5 in dichloroethane, dye III, ( $\tau = 2.7$  ps) produces a mean pulse duration of 1.7 ps.

vent) reproducible single pulse operation was found. When dye III ( $\tau \approx 2.7$  ps) was used in the contacted dye cell, lasing was observed at a high pumping level, but no mode-locking was found at the available pumping power. Mode-locking was observed when dye III was placed between the curved mirrors where the intensity increase was higher. With careful adjustment it was possible to have single-pulse operation at the beginning of the pulse train where the measured pulse was selected.

In this configuration the different dyes are studied. We used the same single-pass low intensity transmission of 80%. The supplied pumping energy was adjusted to optimize single pulse operation. For dye III we obtained the shortest pulse duration  $t_p = 1.7 \pm 0.15$  ps, whereas the commonly used dye I ( $\tau = 7$  ps) produced pulses with  $t_p = 3.2 \pm 0.2$  ps. When we studied dye II ( $\tau = 4.7$  ps) a somewhat shorter pulse duration of  $t_p = 2.5 \pm 0.2$  ps was found. Of interest for the experimental application is the shot-to-shot variation of the pulse duration. We plotted in Fig. 6 two histograms for 72 consecutive shots for dye I (Fig. 6a) and for dye III (Fig. 6b). 70% of all pulses have durations within 0.3 ps around the mean pulse duration.

Finally, we compare the experimental pulse durations with results from our calculations. Figure 7 shows the measured and calculated pulse durations as a function

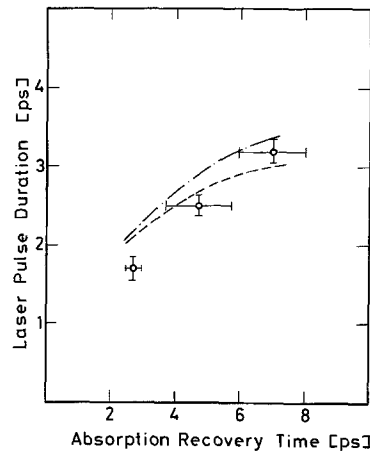


Fig. 7. Pulse durations as a function of the dye absorption recovery time. The experimental points are obtained for dye I ( $\tau = 7$  ps), dye II ( $\tau = 4.7$  ps), and dye III ( $\tau = 2.7$  ps). The theoretical curves are calculated with constant absorption cross section  $\sigma_a = 3.7 \times 10^{-16}$  cm<sup>2</sup>.

of the switching time of mode-locking dyes. Between the two lines we find single-pulse operation. Experiment and theory show the reduction of the pulse duration when the dye with the shorter relaxation time  $\tau$  is used. The reduction is more pronounced in the experiment. A complete agreement is not expected since the absorption cross sections of the various dyes are not known with sufficient accuracy.

In conclusion we wish to emphasize that the presented model allows to simulate the operation of a mode-locked Nd-glass laser. Pulse durations of 1.7 ps are obtained in the experiment when a new mode-locking dye with a time constant of  $\tau = 2.7$  ps is used. The fast switching time,  $\tau \approx t_p$  reduces the duration  $t_p$  of the light pulse and, in addition, suppresses satellite pulses.

*Acknowledgement.* The authors acknowledge valuable contributions and stimulating discussions with Professor W. Kaiser.

## References

1. A.J.DeMaria, D.A.Stetser, H.Heynau: Appl. Phys. Lett. **8**, 174-176 (1966);  
D.A.Stetser, A.J.DeMaria: Appl. Phys. Lett. **9**, 118-120 (1966)
2. J.A.Fleck: Phys. Rev. B **1**, 84-100 (1970)
3. H.Statz: J. Appl. Phys. **38**, 4648-4655 (1967);  
R.R.Cubeddu, O.Svelto: IEEE J. QE-**5**, 495-502 (1969)
4. V.S.Letokhov: Sov. Phys. JETP **28**, 562-568 (1969)
5. P.G.Kryukov, V.S.Letokhov: IEEE J. QE-**8**, 766-782 (1972)
6. D. von der Linde: IEEE J. QE-**8**, 328-338 (1972)
7. D.J.Bradley, G.H.C.New, B.Sutherland, S.J.Caughey: Phys. Lett. **28 A**, 532-533 (1969)
8. G.H.C.New: IEEE J. QE-**10**, 115-124 (1974)
9. G.H.C.New: IEEE J. QE-**14**, 642-645 (1978)  
G.H.C.New: Proc. IEEE, **67**, 380-396 (1979)
10. W.H.Glenn: IEEE J. QE-**11**, 8-17 (1975)

11. B.Hausherr, E.Mathieu, H.Weber: IEEE J. QE-9, 445-449 (1973)
12. R.Wilbrandt, H.Weber: IEEE J. QE-11, 186-190 (1975)
13. A.Laubereau, W.Kaiser: Opto-electron. 6, 1-24 (1974)
14. O.Deutschbein, M.Faulstich, W.Jahn, G.Krolla, N.Neuroth: Appl. Opt. 17, 2228-2232 (1978)
15. Schott Gen., Product Information; N.Neuroth: private communication
16. R.C.Eckardt, C.H.Lee, J.N.Bradford: Opto-electron. 6, 67-85 (1974)
17. W.Zinth, A.Laubereau, W.Kaiser: Opt. Commun. 22, 161-164 (1977)
18. A.Laubereau, D.von der Linde: Z. Naturforsch. 25a, 1626-1642 (1970)
19. B.Kopainsky, W.Kaiser, K.H.Drexhage: Opt. Commun. 32, 451-455 (1980)
20. B.Kopainsky, A.Seilmeier, W.Kaiser: In *Picosecond Phenomena II*, ed. by R.Hochstrasser, W.Kaiser, C.V.Shank, Springer Ser. Chem. Phys. 14 (Springer, Berlin, Heidelberg, New York 1980); A.Seilmeier, B.Kopainsky, W.Kaiser: Appl. Phys. 23, 1-7 (1980)
21. J.Jansky, G.Corradi, R.N.Gyuzalian: Opt. Commun. 23, 293-297 (1977)
- C.Kolmeder, W.Zinth, W.Kaiser: Opt. Commun. 30, 453-457 (1979)